Characterization of Dipyridophenazine Complexes of Ruthenium(II): The Light Switch Effect as a Function of Nucleic Acid Sequence and Conformation

Yonchu Jenkins,[‡] Alan E. Friedman,[‡,§] Nicholas J. Turro,[∥] and Jacqueline K. Barton*[,‡]

Division of Chemistry and Chemical Engineering and the Beckman Institute, California Institute of Technology, Pasadena, California 91125, and Department of Chemistry, Columbia University, New York, New York 10027

Received June 11, 1992; Revised Manuscript Received August 24, 1992

ABSTRACT: Spectroscopic parameters for two novel ruthenium complexes on binding to nucleic acids of varying sequences and conformations have been determined. These complexes, $Ru(bpy)_2dppz^{2+}$ and $Ru(phen)_2dppz^{2+}$ (bpy = 2,2′-bipyridine; phen = 1,10-phenanthroline; dppz = dipyrido[3,2:*a*-2′,3′:*c*]-phenazine) serve as "molecular light switches" for DNA, displaying no photoluminescence in aqueous solution but luminescing intensely in the presence of DNA. The luminescent enhancement observed upon binding is attributed to the sensitivity of the excited state to quenching by water; in DNA, the metal complex, upon intercalation into the helix, is protected from the aqueous solvent, thereby preserving the luminescence. Correlations between the extent of protection (depending upon the DNA conformation) and the luminescence parameters are observed. Indeed, the strongest luminescent enhancement is observed for intercalation into DNA conformations which afford the greatest amount of overlap with access from the major groove, such as in triple helices. Differences are observed in the luminescent parameters between the two complexes which also correlate with the level of water protection. In the presence of nucleic acids, both complexes exhibit biexponential decays in emission. Quenching studies are consistent with two intercalative binding modes for the dppz ligand from the major groove: one in which the metal–phenazine axis lies along the DNA dyad axis and another where the metal–phenazine axis lies almost perpendicular to the DNA dyad axis. $Ru(bpy)_2dppz^{2+}$ and $Ru(phen)_2dppz^{2+}$ are shown here to be unique reporters of nucleic acid structures and may become valuable in the design of new diagnostics for DNA.

Considerable attention has been given to the design of small molecules that bind to DNA with site selectivity so as to develop novel therapeutics and chemical probes for nucleic acid sites and structures, as well as novel diagnostic agents targeted to double-helical DNA (Pyle & Barton, 1990; Dervan, 1986; Moser & Dervan, 1987; Hecht, 1986; Tullius, 1988). Our laboratory has focused in part on the development of transition-metal complexes as probes of nucleic acid structure (Chow & Barton, 1992; Mei & Barton, 1986; Kirshenbaum et al., 1988; Barton, 1986). We have found that ruthenium complexes serve as very sensitive luminescent reporters of DNA in aqueous solution and may become particularly useful in developing new diagnostics.

Ruthenium complexes are ideally suited for application as sensitive noncovalent probes for polymer structure. The complexes are water-soluble, coordinatively saturated, and inert to substitution. Polypyridyl complexes of ruthenium(II) furthermore are intensely colored owing to a well-characterized, localized metal-to-ligand charge transfer (MLCT) transition (Juris et al., 1988). Importantly, this transition is perturbed on binding to DNA, providing a sensitive spectroscopic handle for interactions with nucleic acids (Pyle et al., 1989). Tris(1,10-phenanthroline)ruthenium(II), $Ru(phen)_3^{2+}$, has been established, primarily via photophysical studies (Barton et al., 1986; Kumar et al., 1985; Pyle et al., 1989), to bind to DNA through two noncovalent modes: (i) a groove-bound mode stabilized by hydrophobic interactions of the ligands with the minor groove of DNA and (2) intercalation in the DNA major groove (Rehmann & Barton, 1990a,b). Each binding interaction is enantioselective; the Δ isomer is favored for intercalation into right-handed helices, whereas the groove-bound interaction favors the Λ isomer. Indeed, Λ-$Ru(DIP)_3^{2+}$, the first spectroscopic probe for Z-DNA (Barton et al., 1984), was developed on the basis of the differential binding of ruthenium enantiomers to right- and left-handed helices through matching the symmetry of the metal complexes to the symmetry of the helices.

Recently, a ruthenium(II) polypyridyl derivative, $Ru(bpy)_2dppz^{2+}$ (bpy = 2,2′-bipyridine; dppz = dipyrido[3,2-*a*:2′,3′-*c*]phenazine), was shown to be a remarkable luminescent light switch for DNA (Friedman et al., 1990, 1991; Hartshorn & Barton, 1992). The dipyridophenazine ligand, compared to the parent phenanthroline, has an extended aromatic surface area which allows for extensive intercalative stacking in DNA; dppz complexes bind avidly to DNA through intercalation [for $Ru(bpy)_2dppz^{2+}$ $\log K \geq 7$; for $Ru(phen)_3^{2+}$ $\log K \sim 4$]. $Ru(bpy)_2dppz^{2+}$ also possesses a unique luminescent characteristic. In aqueous solutions at ambient temperatures the complex shows no photoluminescence; yet in the presence of double-stranded DNA, the complex luminesces intensely. The luminescence enhancement on binding to DNA is $\geq 10^4$, compared to an enhancement of ~20 for ethidium (Le Pecq & Paoletti, 1966).

Here we examine characteristics of the interactions of dppz complexes of ruthenium with DNA and RNA so as to identify the scope and versatility of this new luminescent reporter in probing nucleic acids. In particular, we explore the photophysical properties of $Ru(phen)_2dppz^{2+}$ (**1**) and $Ru(bpy)_2dppz^{2+}$ (**2**) on binding to nucleic acids which differ in sequence and conformation. We find the luminescent parameters to be remarkably sensitive to the DNA structure at the intercalation site and, more specifically, to how the structure protects the dppz ligand from interactions with solvent. These luminescent

* Author to whom correspondence should be addressed.
‡ California Institute of Technology.
§ Present address: Eastman Kodak Co., Rochester, NY 14650.
∥ Columbia University.

0006-2960/92/0431-10809$03.00/0

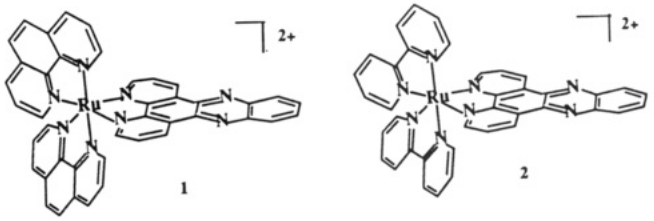

probes may provide unique diagnostic markers for conformation.

MATERIALS AND METHODS

Buffers and Chemicals. All experiments were conducted in deionized, distilled water containing 50 mM NaCl and 5 mM Tris, pH 7.0. Experiments requiring Z-form DNA were carried out in buffer containing 20 mM NaCl, 4 μM $Co(NH_3)_6^{3+}$, and 2 mM Tris, pH 7.0. $RuCl_3 \cdot 3H_2O$ was purchased from Johnson and Matthey/AESAR and $K_4Fe(CN)_6$ from Aldrich Gold Label; both were used without further purification.

Ruthenium Complexes. Tris(2,2′-bipyridyl)ruthenium(II) dichloride was purchased from Aldrich Chemical Co. and used without further purification. The complex bis(2,2′-bipyridyl)(dipyrido[3,2-*a*:2′,3′-*c*]phenazine)ruthenium(II) (hexafluorophosphate), $[Ru(bpy)_2dppz](PF_6)_2$, was prepared as reported previously (Amouyal et al., 1990). Bis(1,10-phenanthroline)(dipyrido[3,2-*a*:2′,3′-*c*]phenazine)ruthenium(II) (hexafluorophosphate), $[Ru(phen)_2dppz](PF_6)_2$, was synthesized using a similar method. An alternate higher yielding synthetic scheme has recently been established (Hartshorn & Barton, 1992).

Nucleic Acids. Polymeric nucleic acids were purchased from Pharmacia as the lyophilized salt. All nucleic acid stock solutions were dialyzed extensively to remove small fragments and to bring them to the appropriate ionic strengths. Yeast $tRNA^{Phe}$ was purchased from Boehringer Mannheim Biochemicals and dissolved in 10 mM Tris buffer, pH 7.5. The Z conformation of DNA was promoted by the addition of $[Co(NH_3)_6]^{3+}$ to B-form poly(dG·dC)·poly(dG·dC) and characterized through the negative Cotton effect seen at 290 nm in the circular dichroic spectrum (Pohl & Jovin, 1972). Oligonucleotides used in the triple-helix experiments were synthesized using either a Pharmacia gene assembler or an Applied Biosystems DNA synthesizer Model 392 and were purifed using reversed phase HPLC. $MgCl_2$ (10 μM) was added to oligonucleotide solutions to stabilize triple-helix formation (Plum et al., 1990). The triple-helix formation was characterized by melting temperature experiments. Dissociation of the third strand was observed at 50 °C; duplex melting occurred at 90 °C.

Spectroscopic Measurements. All absorption spectra were measured using either a Varian Cary 219 spectrophotometer or a Hewlett-Packard 8450 diode array spectrophotometer. Circular dichroism measurements were made on a JASCO J-500 spectropolarimeter. Luminescence measurements were made on a SLM 8000C fluorimeter. Samples contained a metal/nucleotide ratio of 0.1 and were thermally equilibrated for 10 min in a thermostated sample chamber at 20 °C. Luminescence quantum yields were obtained by direct comparison to a 10 μM $[Ru(bpy)_3]Cl_2$ solution irradiated at 440 nm (Φ = 0.042) (Van Houten & Watts, 1975). Peak integrals were obtained using the SLM software package. Quenching experiments were conducted by adding 5–20-μL aliquots of a 20 mM $[Fe(CN)_6]^{4-}$ stock solution to samples containing 10 μM metal and 100 μM nucleotides in the appropriate buffer. Emission lifetimes were measured using a Lambda Physik LPX-200 XeCl excimer pumped dye laser in the Laser Resource Center of the Beckman Institute, as previously described (Friedman et al., 1991). Each emission decay trace resulted from an average of 500 laser shots. The decay traces were deconvoluted using a nonlinear least-squares minimization program.

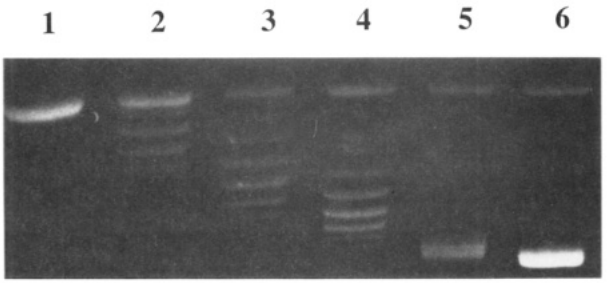

FIGURE 1: Agarose gel showing the unwinding of pBR322 DNA by $Ru(bpy)_2dppz^{2+}$ after incubation with topoisomerase I in the presence of increasing amounts of ruthenium complex. Lanes 1–5 show the topoisomers after incubation of DNA, topoisomerase, and increasing ruthenium concentrations from 3.9 to 8.3 μM. Lane 6 shows DNA without incubation. The gel has been stained with $Ru(bpy)_2dppz^{2+}$.

Topoisomerase Assay. The extent of helix unwinding was determined as described previously (Pyle et al., 1989). Samples were electrophoresed in 0.7% agarose and visualized after incubation for 45 min with 5×10^{-4} M $Ru(bpy)_2dppz^{2+}$; no destaining was required. The unwinding angles were determined from plots of $-\tau$ (the number of superhelical turns) vs the concentration of metal complex according to (Keller, 1975; Waring, 1970)

$$\sigma = -20r_c(\Phi/360) = -r_c\Phi/18$$

where σ is the superhelical density of the plasmid, r_c equals the amount of metal complex ions bound per nucleotide when all of the superhelices are removed, and Φ is the unwinding angle. On the basis of the equilibrium dialysis experiments, added ruthenium concentrations in this assay could be assumed to be totally bound.

RESULTS AND DISCUSSION

Unwinding of Supercoiled DNA. The extent of DNA helix unwinding by a noncovalently bound species may be quantitated by examining the change in superhelical density in a plasmid after relaxation of the plasmid in the presence of bound complex with topoisomerase I (Keller, 1975; Waring, 1970; Kelly et al., 1985). Figure 1 shows the unwinding of pBR322 DNA by $Ru(bpy)_2dppz^{2+}$ following incubation with topoisomerase I in the presence of increasing amounts of ruthenium complex. From these titrations, an unwinding angle of 30 ± 11° per ruthenium bound is obtained for $Ru(bpy)_2dppz^{2+}$. This value is consistent with those observed for other avid intercalating agents such as ethidium bromide (26°) (Keller, 1975) and $Ru(phen)_2phi^{2+}$ (26°) (Pyle et al., 1989).

It should be noted that the agarose gel displaying the unwinding of pBR322 (Figure 1) has been visualized using $Ru(bpy)_2dppz^{2+}$ as a luminescent stain. The luminescence enhancement therefore is also clearly evident in gels. Some comparison to the commonly used stain ethidium may be made. Since for the ruthenium complexes the luminescent enhancement upon DNA binding is $\geq 10^4$, compared to an enhancement of ~20 for ethidium bromide (Le Pecq & Paoletti, 1966), there is essentially no background with the dppz complexes, and no destaining is needed. The dppz complex would

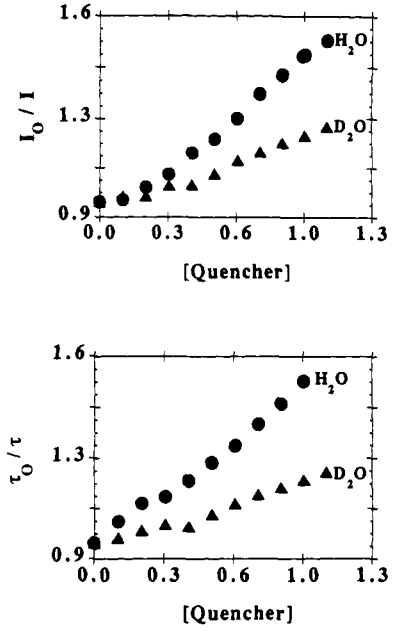

FIGURE 2: Stern–Volmer plots for steady-state (top) and time-resolved (bottom) luminescence quenching of 10 μM $Ru(phen)_2dppz^{2+}$ in acetonitrile by H_2O (circles) and D_2O (triangles).

therefore be used advantageously in instances requiring higher contrast (low background). The luminescence quantum yield for the ruthenium complexes is, however, lower than for ethidium, so that experiments requiring high signal would likely benefit more from application of ethidium. This feature should be kept in mind for future applications.

The results indicate (i) unwinding of the DNA helix and (ii) a luminescent change on binding to DNA. Earlier studies (Friedman et al., 1990, 1991) also indicated (iii) the maintenance of polarization in emission on excitation with polarized light and (iv) the increase in binding affinity for the dppz complex with its extended aromatic framework compared to that for $Ru(phen)_3^{2+}$. These studies collectively support the assignment of binding of the complex to double-helical DNA through intercalation (Long & Barton, 1990).

Quenching by Water of the Luminescent Excited State. The light switch effect of the dppz complexes upon intercalation has been attributed to the protection of the phenazine nitrogen atoms from interaction with water in the intercalated form compared to free in aqueous solution. Electrochemical and photophysical measurements of $Ru(bpy)_2dppz^{2+}$ in both its ground and excited states show that the charge transfer is localized onto the phenazine ligand (Chambron et al., 1985; Amouyal et al., 1990). In addition, comparisons of binding affinities for a series of mixed ligand intercalating complexes show that for mixed phenanthroline or bipyridyl complexes of dppz, it is the dppz ligand that intercalates and thus would be protected (Pyle et al., 1989). To establish that the quenching of the ruthenium excited state is indeed the result of interactions with water, we examined the quenching of the excited state of the complex by water in a nonaqueous solvent.

Figure 2 shows a Stern–Volmer plot for luminescence quenching of $Ru(phen)_2dppz^{2+}$ in acetonitrile with increasing concentrations of H_2O and D_2O. Addition of D_2O also quenches the emission of the complex but at a slower rate. The isotope effect, k_H/k_D, of 2.1 supports the notion of quenching through vibrational deactivation via a hydrogen bonding pathway (Lin & Struve, 1991). Luminescence quenching can also be followed using time-resolved techniques. Table I shows the excited-state lifetimes for the dppz complexes in nonaqueous solvent and intercalated into calf thymus DNA. Time-resolved quenching studies of $Ru(phen)_2dppz^{2+}$ by H_2O and D_2O resulted in a similar k_H/k_D of 2.2. It is noteworthy that the ratio of the luminescence of the intercalated complex in calf thymus DNA relative to $Ru(bpy)_3^{2+}$ is 0.94, compared to 0.57 in dry acetonitrile. Hence, the intercalation environment completely protects the dppz ligand from interactions with water, as in a nonaqueous system; likely in addition, as with $Ru(phen)_3^{2+}$, the intercalated complex is also rigidly held in the DNA helix, increasing its luminescence still further relative to that in nonaqueous solution. These results are consistent with the proposed mechanism for the light switch effect.

Anionic Quenching of Ruthenium Complexes in the Presence of DNA. As is evident in Table I, upon intercalation into B-DNA, a biexponential decay in emission is observed for both dppz complexes, indicating the presence of two distinguishable DNA binding modes for the complexes. One might consider that the bound enantiomers show decays in emission at different rates. Given that in the racemate both enantiomers of $Ru(phen)_2dppz^{2+}$ are fully bound to the DNA in these experiments and that the percentage of each component of the emission decay is not 50%, the biexponential decay for the bound racemate cannot, however, be attributed to differential binding by enantiomers. Photophysical studies on the parent complex, $Ru(phen)_3^{2+}$, bound to calf thymus DNA also indicated biphasic decays in emission which were attributed to two different binding modes; for the intercalative interaction the excited-state lifetime of $Ru(phen)_3^{2+}$ is increased from 0.6 to 2 μs [no difference in emission decay rate has been found between intercalatively bound enantiomers of $Ru(phen)_3^{2+}$], while for the groove-bound interaction, the excited-state lifetime is comparable to that of the free form. These two modes were assigned in part through quenching studies using anionic quenchers such as $Fe(CN)_6^{4-}$ which quenches the groove-bound form with an efficiency less than that of free ruthenium (owing to the association of the groove-bound species with the DNA polyanion) but which does not quench the closely bound intercalated form (Kumar et al., 1985). Quenching of the excited state using an anionic quencher therefore permits the discrimination between differently bound ruthenium species.

In an effort to characterize the biexponential decay characteristics of the dppz complexes, time-resolved quenching experiments with ferrocyanide were therefore also conducted. Figure 3 shows the results for $Ru(phen)_2dppz^{2+}$ with $Ru(phen)_3^{2+}$ as a comparison. As can be seen in the figure, no quenching of the $Ru(phen)_2dppz^{2+}$ excited state by $Fe(CN)_6^{4-}$ is evident, even after the addition of a 50-fold excess of the quencher; an analogous result is apparent with $Ru(bpy)_2dppz^{2+}$. With $Ru(phen)_3^{2+}$, in contrast, quenching of one component of its biexponential decay in emission, that assigned to the surface-bound mode, is apparent. These results indicate that with the dppz complexes both lifetimes correspond to modes where the complex is embedded in the interior of the helix, inaccessible to the quencher. The results therefore suggest that for these dppz complexes both binding modes may be intercalative.

The absence of a significant surface-bound mode for the dppz complexes is not surprising, given the large increase in binding affinity for the dppz complexes compared to that of $Ru(phen)_3^{2+}$. What is unusual is our ability to detect using photophysical methods the presence of two different intercalative associations with the helix. On the basis of photophysical studies of various dppz derivatives (where the dppz

Table I: Emission Characteristics of $[RuL_2dppz]^{2+}$ in Nonaqueous Solvent and Intercalated into Calf Thymus DNA[a]

	$[Ru(bpy)_2dppz]^{2+}$				$[Ru(phen)_2dppz]^{2+}$			
solvent/nucleic acid	τ[b] (ns)	%[c]	λ_{max}[b] (nm)	RI[d]	τ[b] (ns)	%[c]	λ_{max}[b] (nm)	RI[d]
acetonitrile	180		622	0.54	180		619	0.57
calf thymus DNA	340	20	621	0.16	770	40	617	0.94
	90	80			120	60		

[a] All measurements were conducted at 20 °C using 10 μM ruthenium/100 μM nucleotides and excitation at 440 nm. [b] Error is estimated to be ±10% for both steady-state and time-resolved measurements. [c] The percentage of each component of the biexponential emission decay was calculated from the magnitudes of the preexponential factors produced by the fitting program. [d] Relative emission intensities (RI) were determined as a ratio of emission relative to a 10 μM $[Ru(bpy)_3]^{2+}$ solution.

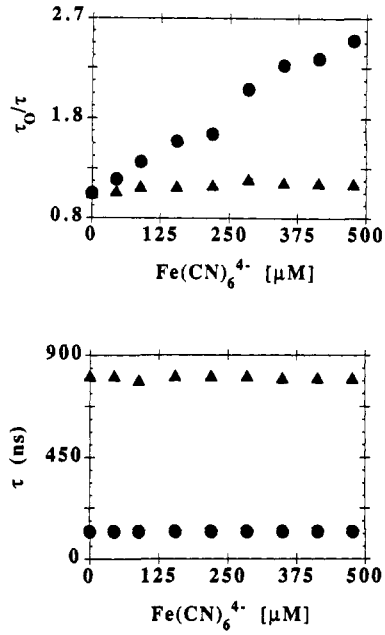

FIGURE 3: Luminescent quenching of the long-lived component (triangle) and short-lived component (circle) for 10 μM $Ru(phen)_3^{2+}$ (top) and $Ru(phen)_2dppz^{2+}$ (bottom) in the presence of 100 μM calf thymus DNA by $[Fe(CN)_6]^{4-}$. The quenching is plotted in Stern–Volmer form for $Ru(phen)_3^{2+}$ and shows the surface-bound form to be quenched, while the intercalatively bound component is more difficult to quench. In the case of $Ru(phen)_2dppz^{2+}$, the plot shows no variation in luminescence for either component as a function of added quencher, consistent with the assignment of both components as intercalative.

ligand has been substituted in either symmetric or asymmetric fashion), two specific intercalative binding modes have been proposed (Hartshorn & Barton, 1992): (i) a perpendicular mode where the dppz ligand intercalates from the major groove such that the metal–phenazine axis lies along the dyad axis and (ii) a side-on mode where the dppz ligand intercalates so that the metal–phenazine axis lies more closely to the long axis of the base pairs.

Variation in Emission Characteristics with Sequence. Summarized in Table II are the changes in steady-state luminescence and time-resolved parameters observed upon binding to AT- vs GC-containing synthetic polymers by $Ru(bpy)_2dppz^{2+}$ and $Ru(phen)_2ddpz^{2+}$. A difference is clearly evident. The maximum wavelength for emission ranges from 620 to 624 nm for AT sequences and from 606 to 610 nm for GC sequences. Results with calf thymus DNA are intermediate (but closer to those of the AT-rich DNA). It is not surprising that the emission is sensitive to the base-pair site surrounding the phenazine ligand. This trend is reinforced by the differences in excited-state lifetimes of the dppz complexes bound to the polymers which differ in sequence. Complexes bound to AT sequences display longer excited-state lifetimes (~300–800 ns) than do GC sequences (~200–400 ns). Differences are evident, however, beyond the base composition of the site. It is interesting that, among the different sequences, the longest excited-state lifetimes are observed with poly(dA)·poly(dT), which is considered (Kennard & Hunter, 1989) to be the structure of greatest stiffness among the synthetic variations.

Variation in Emission Characteristics with Double-Helical Conformation. Table III shows the variation in steady-state luminescence and time-resolved parameters by $Ru(bpy)_2ddpz^{2+}$ and $Ru(phen)_2dppz^{2+}$ as a function of nucleic acid conformation. Both the relative intensity of emission and the rate of decay in emission appear to be quite sensitive to the overall nucleic acid conformation. Highest luminescence is evident with triple-helical DNA, followed by Z- and B-form helices, with lower luminescence evident with the A conformation. Equilibrium dialysis experiments (data not shown) with double-helical synthetic polymers furthermore indicate a corresponding trend of high binding for Z- and B-DNA, with lower affinity for A-form RNA.

Emission intensity is seen to be lowest for the A-form double helices, poly[r(AU)]·poly[r(AU)] and poly(rG)·poly(dC). With $Ru(bpy)_2dppz^{2+}$, the emission intensity is ~4% of that observed with its deoxyribose B-form analogue. In A-form helices, the base pairs are pushed back toward the periphery of the double helix, resulting in a very deep and narrow major groove (Saenger, 1984). The shape of this cavity renders it inaccessible to intercalation from the major groove by $Ru(phen)_3^{2+}$ (Barton et al., 1986), and likely a similar difficulty is apparent even with the longer dppz ligand. It is surprising that intercalation, or a partial protection, even occurs at all with the A form, showing the avidity of binding for dppz complexes. The differential effect is less pronounced but clear with $Ru(phen)_2dppz^{2+}$ [13% relative intensity with poly[r(AU)]·poly[r(AU)] compared to poly[d(AT)]·poly[d(AT)]]. The lowered sensitivity likely reflects how efficiently the ancillary ligands protect the dppz in the groove from access of water (vide infra). The overall differences apparent with the A form compared to B-DNA also support intercalation by these ruthenium complexes from the major groove; other metallointercalators had been shown to bind DNA from the major groove using crystallography (Wang et al., 1978) and in DNA cleavage experiments (Sitlani et al., 1992).

Substantial luminescence is apparent on binding to Z-form polymers, consistent with an "intercalative interaction" for the dppz complexes in Z-DNA as well as B-DNA. Earlier studies comparing a range of spectroscopic parameters for ruthenium(II) complexes, notably $Ru(phen)_3^{2+}$ enantiomers, on binding B- vs Z-DNA have indicated that an intercalative binding may occur for metallointercalators with a Z-form helix (Friedman et al., 1991), compared to other intercalators which promote transitions back to the B form. Likely the association of the dppz complexes of ruthenium in the major groove of DNA stabilizes the Z-form helix. It must be noted that since the transition to the Z form requires the addition of cobalt hexaammine, we have included as a control the

Table II: Emission Characteristics of $[RuL_2dppz]^{2+}$ upon Binding to AT- vs GC-Containing Synthetic Polymers[a]

	$[Ru(bpy)_2dppz]^{2+}$				$[Ru(phen)_2dppz]^{2+}$			
nucleic acid	τ[b] (ns)	%[c]	λ_{max} (nm)	RI[d]	τ[b] (ns)	%[c]	λ_{max}[b] (nm)	RI[d]
poly[d(GC)]·poly[d(GC)]	220	60	610	0.29	290	60	606	0.61
	70	40			70	40		
poly(dG)·poly(dC)	260	30	610	0.29	400	40	607	0.74
	70	70			90	60		
poly[d(AT)]·poly[d(AT)]	320	20	624	0.17	740	40	620	0.75
	90	80			120	60		
poly(dA)·poly(dT)	340	40	626	0.23	840	60	621	1.39
	80	60			110	40		

[a] All measurements were conducted at 20 °C using 10 μM ruthenium/100 μM nucleotides and excitation at 440 nm. [b] Error is estimated to be ±10% for both steady-state and time-resolved measurements. [c] The percentage of each component of the biexponential emission decay was calculated from the magnitudes of the preexponential factors produced by the fitting program. [d] Relative emission intensities (RI) were determined as a ratio of emission relative to a 10 μM $[Ru(bpy)_3]^{2+}$ solution.

Table III: Emission Characteristics of $[RuL_2dppz]^{2+}$ upon Binding to Nucleic Acids of Varying Conformations[a]

	$[Ru(bpy)_2dppz]^{2+}$				$[Ru(phen)_2dppz]^{2+}$			
nucleic acid	τ[b] (ns)	%[c]	λ_{max}[b] (nm)	RI[d]	τ[b] (ns)	%[c]	λ_{max}[b] (nm)	RI[d]
poly[d(G-m^{5}C)]·poly[d(G-m^{5}C)]	240	40	606	0.25	360	40	606	0.51
	60	60			90	60		
Z-poly[d(GC)]·poly[d(GC)]	220	60	608	0.28	270	60	608	0.60
	70	40			70	40		
calf thymus DNA Z conditions	330	40	621	0.21	750	40	616	0.80
	80	60			120	60		
poly[r(AU)]·poly[r(AU)][e]	400	10	626	0.0057	490	20	620	0.10
	50	90			80	80		
poly(rG)·poly(dC)[e]	540	10	620	0.0067	520	30	616	0.04
	70	90			80	70		
100 μM poly(dT)·poly(dA)·poly(dT)[f]	430	70	621	0.60	530	60	621	1.45
	170	30			170	40		
$tRNA^{Phe}$	300	30	624	0.06	300	30	620	0.18
	60	70			70	70		

[a] All measurements were conducted at 20 °C using 10 μM ruthenium/100 μM nucleotides and excitation at 440 nm. [b] Error is estimated to be ±10% for both steady-state and time-resolved measurements. [c] The percentage of each component of the biexponential emission decay was calculated from the magnitudes of the preexponential factors produced by the fitting program. [d] Relative emission intensities (RI) were determined as a ratio of emission relative to a 10 μM $[Ru(bpy)_3]^{2+}$ solution. [e] Error in time-resolved measurements for A-form polynucleotides is more uncertain than 10% given the low overall luminescent intensity. [f] 10 μM Mg^{2+} was added to stabilize triplex formation.

spectroscopic parameters for calf thymus DNA, still primarily in the B form, in the presence of cobalt hexaammine.

Also included are the luminescent parameters for poly-[d(G-m^{5}C)]·poly[d(G-m^{5}C)], which in the B form shows small but significant decreases in luminescent intensity on binding by the dppz complexes compared to B-form poly[d(GC)]·poly-[d(GC)]. Since the methyl group protrudes from the major groove, this decrease in intensity is consistent also with the perturbed access of the complexes upon intercalation from the major groove.

Binding to a Triple Helix. Table III includes the luminescent parameters for binding of $Ru(bpy)_2dppz^{2+}$ and $Ru(phen)_2dppz^{2+}$ to a triple-helical conformation. As may be evident from the table, the highest luminescent intensities with $Ru(bpy)_2dppz^{2+}$ and longest excited-state lifetimes are observed upon binding to the triple-helical conformation. This effect is substantially more pronounced upon binding of the bpy derivative in comparison to $Ru(phen)_2dppz^{2+}$. The increased lifetime is in part the result of association with the AT sequence. However, in addition, this substantial protection with a triple helix for the dppz ligand from water is understandable given the extended surface area for stacking of a triply bonded array. The triple helix, furthermore, in contrast to an A-form helix, may also provide access for stacking from the major groove (Chow et al., 1992).

Figure 4 schematically illustrates luminescence experiments to test whether intercalative binding by $Ru(bpy)_2dppz^{2+}$ occurs within the triple-helical region or possibly instead at the junction of the triple-helical segment with the duplex. It was

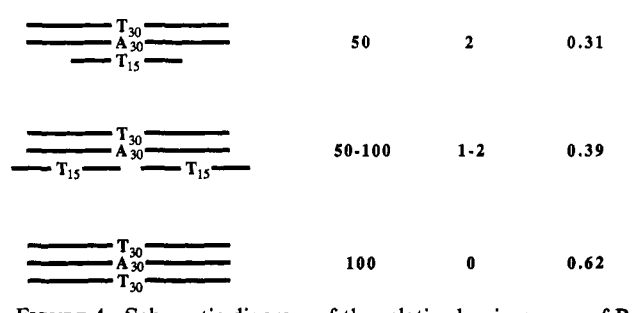

FIGURE 4: Schematic diagram of the relative luminescence of $Ru(bpy)_2dppz^{2+}$ bound to different oligomers. The luminescent intensity correlates with the percentage of triple helix in these oligomeric mixtures, rather than with the number of junctions bordering triple-helical regions, and indicates the greatest luminescence of the ruthenium complex upon intercalation into the triple-helical region.

recently demonstrated that the intercalator ethidium bromide also binds to a triple helix (Mergny et al., 1991; Scaria & Shafer, 1991). Other planar aromatic chromophores such as ellipticine (Perroualt et al., 1990) and acridine (Collier et al., 1991) have been reported to intercalate exclusively at the triplex–duplex junction, rather than within the triple helix itself, indicating the presence of an altered conformation at the junction which creates a strong binding site for these planar aromatic chromophores. We therefore compared luminescence intensity for $Ru(bpy)_2dppz^{2+}$ in the presence of $d(A)_{30}$·d-

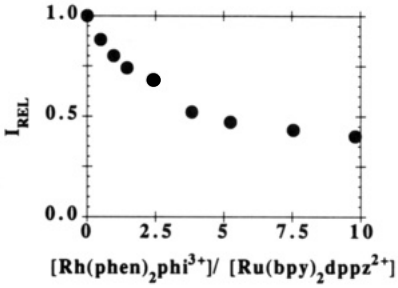

FIGURE 5: Plot showing the relative luminescence of Ru(bpy)$_2$dppz^{2+} (10 μM) bound to tRNA^{Phe} (720 μM nucleotides) as a function of increasing concentration of Rh(phen)$_2$phi^{3+}.

(T)$_{30}$ to which was added either 1 equiv of d(T)$_{15}$, 2 equiv of d(T)$_{15}$, or 1 equiv of d(T)$_{30}$. Upon triple-helix formation with only 1 equiv of d(T)$_{15}$, two junctions would be present and at most 50% of the steps on the oligomer complex would represent intercalation sites. With d(T)$_{30}$, essentially all sites would be triple-helical and lacking in junctions with a duplex. With the addition of 2 equiv of d(T)$_{15}$, statistically both the number of triple-helical steps and the number of junctions would be intermediate between the two extremes. The greatest luminescence is clearly evident with d(T)$_{30}$·d(A)$_{30}$·d(T)$_{30}$, which demonstrates that it is the triple-helical sites rather than the junctions that contribute to the luminescence. A similar but again less pronounced effect is evident with Ru(phen)$_2$dppz^{2+}.

Binding to tRNA^{Phe}. As may be seen in Table III, binding to a folded RNA such as tRNA^{Phe} yields greater luminescence than is observed with a double-helical A-form polymer such as poly[r(AU)]·poly[r(AU)]. This observation suggests that the dppz complexes bind to alternate sites on the folded tRNA. To test this notion, a competitive binding experiment was conducted using Rh(phen)$_2$phi^{3+}, which has been shown to bind specificially to sites of tertiary interaction on tRNA^{Phe} (Chow & Barton, 1990, 1992). Figure 5 shows this competition experiment. With added rhodium complex, which itself does not luminesce, the luminescence of the bound Ru(bpy)$_2$dppz^{2+} is seen to decrease, but only to approximately 30% of its original value. This result would suggest that at least one but not all sites of binding by the dppz complex on tRNA^{Phe} overlap with the tertiary sites targeted by Rh(phen)$_2$phi^{3+}. This result is furthermore consistent with the observation, described above, of enhanced luminescence upon association with triple-helical DNA sites.

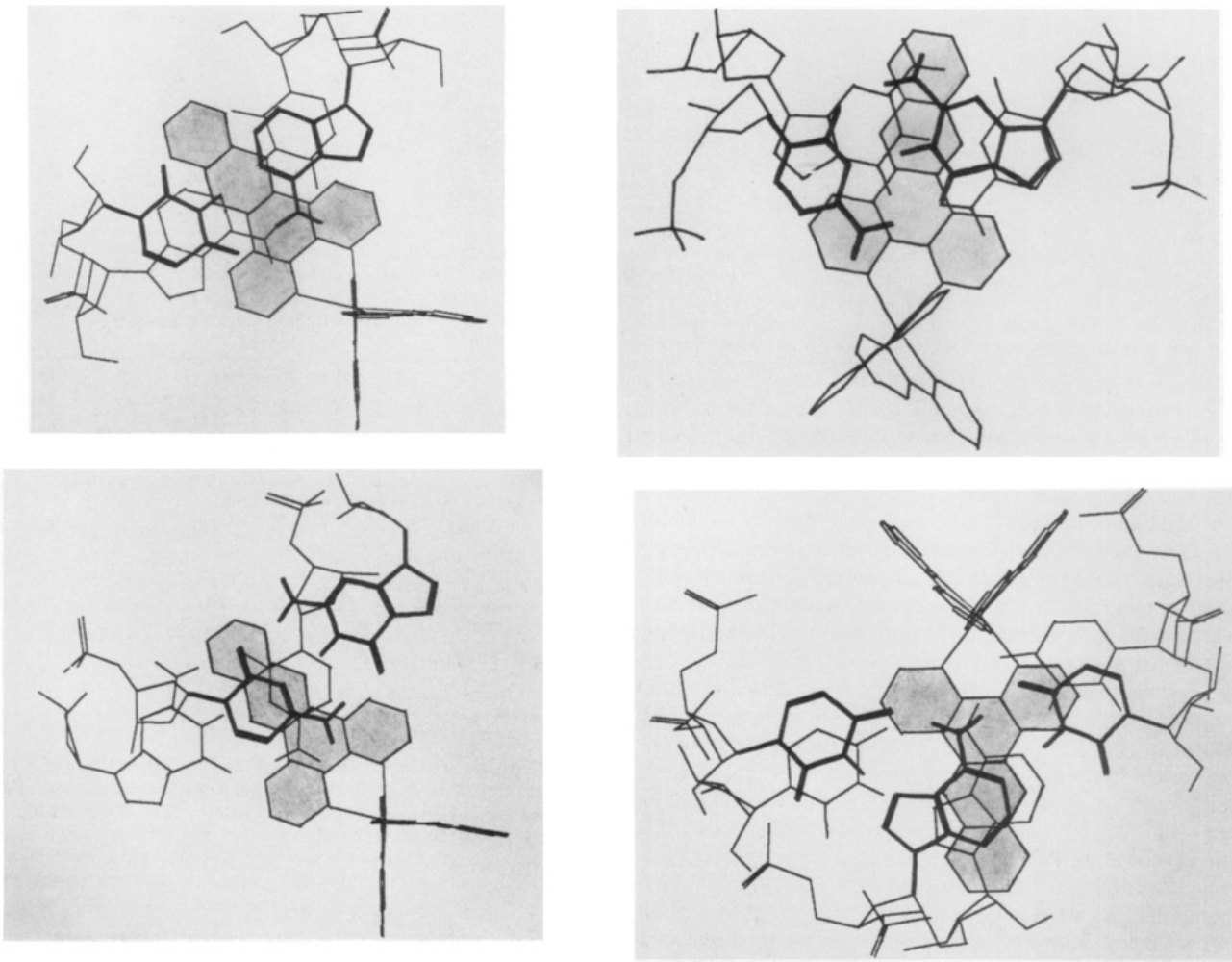

FIGURE 6: Models, looking down the helix axis, which illustrate possible intercalation by the dppz complex into the major groove of the A (A, upper left) B (B, upper right), and Z (C, lower left) forms as well as into a triple-helical (D, lower right), conformation to show the varying degrees of overlap of the base pairs (or triples) in the different nucleic acid conformations with the intercalated dppz complex. With the B, Z, and triple-helical conformations, more protection of the phenazine ring by the bases stacked above and below may be evident. The B-form structure was generated using crystal structure data from a dinucleotide intercalation site (Wang et al., 1978). Intercalation sites for the other conformations were constructed by building a dinucleotide using known helical parameters (Saenger, 1984) and rotating the top base pair or triple in the opposite direction (of helix winding) by 10° around the helix axis (26° unwinding angle for the intercalator). Graphics were generated using MACROMODEL. These models illustrate how stacking of the dppz complex into the different conformations might provide different levels of protection of the phenazine nitrogen atoms from water. The greatest extent of protection and most substantive overlap is clearly with the triple-helical array.

Comparison of Luminescent Parameters for $Ru(phen)_2dppz^{2+}$ and $Ru(bpy)_2dppz^{2+}$. The relative luminescence intensity and excited-state lifetime with each polynucleotide are consistently seen to be greater for $Ru(phen)_2dppz^{2+}$ than for $Ru(bpy)_2dppz^{2+}$. In fact, it is the value of the long-lifetime component that is found to vary substantially between the complexes, whereas the short lifetimes are always similar in magnitude. The difference in these parameters therefore depends sensitively upon the ancillary ligands. The ancillary phenanthrolines are larger than the bipyridines, certainly yielding a greater aromatic surface and increased hydrophobicity. The increased size and hydrophobicity of the phenanthroline ligand must affect the ability of the ligands to shield the dppz ligand from water, thereby preserving the emission resulting from the MLCT excited state. Bipyridines also shield the dppz ligand from water but not to the same extent. Because the ancillary bipyridines are not as efficient in shielding as are the phenanthrolines, the luminescence of the bpy derivative becomes a more sensitive source of discrimination between sites and conformations. Perhaps the greater torsional flexibility of the bipyridyl ring compared to phenanthroline contributes to the lower efficiency in shielding as well.

The fact that substantial differences between complexes are seen in the longer-lived excited-state component and not the short-lifetime component also supports our assignments of perpendicular and side-on models for intercalation. In the side-on model, because the ancillary ligands are canted toward one side of the groove, they should both be equally ineffective at protecting the exposed phenazine nitrogen from water. Consequently, there is only a slight variation in the short lifetimes for the two complexes. For the perpendicular mode, which corresponds to the longer lived excited-state component, differences in extents of water protection, owing to shielding by the differently sized ancillary ligands, would be expected.

Correlation of Conformational Luminescence Parameters with Water Protection. Figure 6 shows a model to illustrate how the different conformations may fix the overlap between the base pairs (or triples) and the intercalated complex. The model was constructed with the constraint of no internuclear distances of <3 Å between the metal complex and DNA. Since structural information is available only for intercalation into a B-form site, for the purposes of considering luminescence parameters with various conformations, we have assumed an analogous intercalation and we have unwound (in the opposite sense for the Z site) the base-pair (triple) sites 10° from the starting conformation (yielding a 26° unwinding angle for the intercalator) so as to accommodate an intercalator. Models have only been constructed for the perpendicular binding mode. One can see the appropriate matching of surface areas for the dppz ligand with a B conformation, where bases stacked above and below the dppz ligand serve to shield the phenazine nitrogen atoms from water. In the case of the A conformation, if reasonable overlap is established with the base pair above (as viewed in Figure 6A), then poor protection of the phenazine ring by the base pair below is observed. This relatively poor protection correlates with the low relative luminescent intensities found with the A conformation. With the Z-helix model, comparable protection by the base pairs above and below in the intercalation site may be obtained. Most extensive overlap of the dppz ligand is evident with a triple-helical arrangement, since now the extended surface area of the base triple completely surrounds the intercalating ligand; with the triple helix, the highest level of luminescence is observed. The luminescence data, therefore, viewed in the context of these overlap models, point to a basic correlation of relative luminescence and excited-state lifetime with how well the given conformation serves to protect the phenazine ligands from water accessibility.

Conclusions. $Ru(bpy)_2dppz^{2+}$ and $Ru(phen)_2dppz^{2+}$ have been shown to be extremely sensitive luminescent probes of nucleic acids, since the complexes, which show no emission in aqueous solution, luminesce intensely upon intercalation in duplex DNA. This molecular light switch effect is seen to depend upon the protection of the phenazine ligand from water that occurs with intercalation of the complex into the helix. The level of water protection and hence luminescent properties of the complexes are sensitive to the nucleic acid conformation. Indeed, the highest level of emission is observed upon binding to triple-helical DNA, where substantial overlap and stacking between the dppz ligand and base triple likely occurs. The variations in luminescence properties also indicate aspects of the binding orientations of the dppz complexes on the helix. The luminescence data are consistent with two intercalative binding modes: one in which the metal–phenazine axis lies along the DNA dyad axis and another in which the metal–phenazine axis is perpendicular to the DNA dyad axis. These intercalative interactions appear furthermore to arise in the major groove of DNA. The dipyridophenazine complexes of ruthenium(II) therefore represent novel reporters of nucleic acid sites and structures and hence may be valuable in the design of new diagnostic and imaging agents.

ACKNOWLEDGMENT

We are grateful to the NIH (GM33309 and an NIH traineeship to Y.J.) for their support of this research.

REFERENCES

Amouyal, E., Homsi, A., Chambron, J. C., & Sauvage, J. P. (1990) *J. Chem. Soc. Dalton Trans.*, 1841–1845.
Barton, J. K. (1986) *Science 233*, 727–734.
Barton, J. K., Basile, L. A., Danishefsky, A., & Alexandrescu, A. (1984) *Proc. Natl. Acad. Sci. U.S.A. 81*, 1961–1965.
Barton, J. K., Goldberg, J. M., Kumar, C. V., & Turro, N. J. (1986) *J. Am. Chem. Soc. 108*, 2081–2090.
Chambron, J.-C., Sauvage, J.-P., Amouyal, E., & Koffi, P. (1985) *New J. Chem. 9*, 527–529.
Chow, C. S., & Barton, J. K. (1990) *J. Am. Chem. Soc. 112*, 2839–2841.
Chow, C. S., & Barton, J. K. (1992) *Methods Enzymol. 212*, 219–241.
Chow, C. S., Behlen, L. S., Uhlenbeck, O. C., & Barton, J. K. (1992) *Biochemistry 31*, 972–982.
Collier, D. A., Mergny, J., Thuong, N., & Helene, C. (1991) *Nucleic Acids Res. 19*, 4219–4224.
Dervan, P. B. (1986) *Science 232*, 464–471.
Friedman, A. E., Chambron, J.-C., Sauvage, J.-P., Turro, N. J., & Barton, J. K. (1990) *J. Am. Chem. Soc. 112*, 4960–4962.
Friedman, A. E., Kumar, C. V., Turro, N. J., & Barton, J. K. (1991) *Nucleic Acids Res. 19*, 2595–2602.
Hartshorn, R. M., & Barton, J. K. (1992) *J. Am. Chem. Soc. 114*, 5919–5925.
Hecht, S. M. (1986) *Acc. Chem. Res. 19*, 383–391.
Juris, A., Balzani, V., Barigelletti, F., Campagna, S., Belser, P., & Von Zelewsky, A. (1988) *Coord. Chem. Rev. 84*, 85–277.
Keller, W. (1975) *Proc. Natl. Acad. Sci. U.S.A. 72*, 4876–4880.
Kelly, J. M., Tossi, A. B., McConnell, D. J., & OhUigin, C. (1985) *Nucleic Acids Res. 13*, 6017–6034.
Kennard, O., & Hunter, W. H. (1989) *Q. Rev. Biophys. 22*, 327–379.
Kirshenbaum, M. R., Tribolet, R., & Barton, J. K. (1988) *Nucleic Acids Res. 16*, 7943–7960.
Kumar, C. V., Barton, J. K., & Turro, N. J. (1985) *J. Am. Chem. Soc. 107*, 5518–5523.

Le Pecq, J.-B., & Paoletti, C. (1966) *Anal. Biochem. 17*, 100–107.
Lin, S., & Struve, W. S. (1991) *Photochem. Photobiol. 54*, 361–365.
Long, E. C., & Barton, J. K. (1990) *Acc. Chem. Res. 23*, 271–273.
Mei, H. Y., & Barton, J. K. (1986) *J. Am. Chem. Soc. 108*, 7414–7416.
Mergny, J. L., Collier, D., Rougee, M., Montenay-Garestier, T., & Helene, C. (1991) *Nucleic Acids Res. 19*, 1521–1526.
Moser, H. E., & Dervan, P. B. (1987) *Science 238*, 645–650.
Perroualt, L., Asseline, U., Rivalle, C., Thuong, N. T., Bisagni, E., Giovannangeli, C., Le Doan, T., & Helene, C. (1990) *Nature 344*, 358–360.
Plum, G. E., Park, Y., Singleton, S. F., Dervan, P. B., & Breslauer, K. J. (1990) *Proc. Natl. Acad. Sci. U.S.A. 87*, 9436–9440.
Pohl, F. M., & Jovin, T. M. (1972) *J. Mol. Biol. 67*, 375–396.
Pyle, A. M., & Barton, J. K. (1990) *Prog. Inorg. Chem. 38*, 413–475.
Pyle, A. M., Rehmann, J. P., Meshoyrer, R., Kumar, C. V., Turro, N. J., & Barton, J. K. (1989) *J. Am. Chem. Soc. 111*, 3051–3058.
Rehmann, J. P., & Barton, J. K. (1990a) *Biochemistry 29*, 1701–1709.
Rehmann, J. P., & Barton, J. K. (1990b) *Biochemistry 29*, 1710–1717.
Saenger, W. (1981) in *Principles of Nucleic Acid Structure* (Cantor, C. R., Ed.) pp 220–241, Springer-Verlag, New York.
Scaria, P. V., & Shafer, R. H. (1991) *J. Biol. Chem. 266*, 5417–5423.
Sitlani, A., Long, E. C., Pyle, A. M., & Barton, J. K. (1992) *J. Am. Chem. Soc. 114*, 2303–2312.
Tullius, T. D. (1988) *Nature 332*, 663–664.
Van Houten, J., & Watts, R. J. (1975) *J. Am. Chem. Soc. 97*, 3843–3844.
Wang, A. H. J., Nathans, J., van der Marel, G., van Boom, J. H., & Rich, A. (1978) *Nature 276*, 471–478.
Waring, M. (1970) *J. Mol. Biol. 54*, 247–279.